The extended time evolution size decrease of gold nanoparticles formed by the Turkevich method

Madeeha A. Uppal,[a] Andreas Kafizas,[a] Teck H. Lim[b] and Ivan P. Parkin*[a]

Received (in Montpellier, France) 10th December 2009, Accepted 15th February 2010
First published as an Advance Article on the web 25th March 2010
DOI: 10.1039/b9nj00745h

Gold nanoparticle (Au NP) solutions were synthesised by the Turkevich reduction method and stored in either the light or dark. All solutions were monitored daily using UV-visible absorption spectroscopy and displayed surface plasmon resonance (SPR), typical of Au nanoparticle colloids. An increase in SPR intensity, a narrowing of the SPR peak as well as a gradual shift towards lower wavenumbers over time indicated a decrease in average nanoparticle diameter and a more mono-dispersed particle size. After two weeks no further changes were observable by UV-visible absorption spectroscopy. A series of high resolution transmission electron micrographs (HRTEM) taken over the evolution period confirmed that the plasmon resonance shifts correlated to a decrease in nanoparticle size. A systematic size decrease in nanoparticle size was also observed for solutions even after centrifugation to remove the excess un-reacted citrate and auric acid. This indicated that the size evolution was independent of further excess reactant chemistries and charge stabilities. The gold nanoparticle evolution followed an inverse Ostwald type growth, by which the size of the NPs decreases, in effect a digestive ripening. The aging process provides a reliable route to fairly mono-dispersed gold nanoparticles of *ca.* 11.5–12.5 nm in size *via* the Turkevich method.

Introduction

Gold nanoparticles (Au NPs) have recently received great interest, principally due to their intense and tuneable surface plasmon resonance (SPR) properties.[1] Current research has employed Au NPs for the enhancement of optical properties in semiconductor thin films *via* composite formation,[2–7] the destruction of bacteria,[8–10] improvements in detection of cancer[11] and DNA[12] and even single molecule detection *via* surface enhanced Raman spectroscopy (SERS).[13,14]

Several methods have been used to produce Au NPs for example sonolysis,[15] laser ablation,[16,17] protein reduction,[18] CVD[19] and more commonly the Brust–Schiffrin reduction,[20] each with associated implications on the size and shape distribution. The method used in this paper was devised by Turkevich *et al.*,[21] which involves the reduction of an auric acid solution by sodium citrate forming predominantly spherical Au NPs.[22]

It has been shown that the SPR of Au NPs is not only size but also shape dependent.[23] Monitoring citrate formed NPs by both UV-visible spectroscopy and transition electron microscopy (TEM) allowed for the derivation of functions relating the SPR peak to average nanoparticle diameter.[24,25] The reaction kinetics of Au NP formation using the citrate method was also recently investigated by Kimling *et al.* for a range of reagent concentrations.[26] The reaction was monitored by UV-visible absorption spectroscopy *in situ* and the NP diameters were predicted. These were found to be in strong agreement with NP diameters determined using X-ray scattering. An Ostwald ripening[27] type growth was observed, whereby particles increased in size over the reaction period of around 50 s and levelled out to a maximum size. Rodriguez-Gonzalez *et al.* synthesised Au nanoparticles *via* the Turkevich method where the solutions were heated more slowly allowing for a slower reaction progression that was monitored spectroscopically, electrochemically and as aliquots by TEM.[27] The reaction took approximately 700 minutes to complete, after 1 minute, large nanoparticle clusters (*ca.* 100 nm) composed of smaller particles (5–10 nm) initially formed. A sharp increase in the conductivity at 600 minutes heating led to the formation of nanoparticles of *ca.* 15 nm in size, concordant with a shift in the SPR band to higher energy. Similar to Chow and Zukoski's conclusions on the mechanism of Turkevich formed nanoparticles, it was surmised that in the early stages of the reduction reaction, only a fraction of the gold salt was consumed and that a complex was formed between gold chloride and citrate/citrate oxidation products.[27] The absorption of $AuCl_4^-$ led to reversible aggregation where citrate absorption occurred at the end of the reaction resulting in a progressive increase in the surface potential. An acceleration in the rate of loss of $AuCl_4^-$ was seen when $[AuCl_4^-/Au^0] = 0.7$ corresponding with a rapid change in the solution colour from light purple to red, and a rapid decrease in size of the large cluster particles seen in TEM.[27]

It is recognized that citrate formed Au NPs are water stable for long periods of time—years; however it is not documented whether changes to particle size, distribution or concentration

[a] *Department of Chemistry, University College London, 20 Gordon Street, London, UK WC1H 0AJ. E-mail: i.p.parkin@ucl.ac.uk; Fax: +44 (0)20 7679 7463; Tel: +44 (0)20 7679 4669*
[b] *Department of Materials, University of Oxford, Parks Road, Oxford, UK OX1 3PH*

occur to this solution. Previous time evolution studies of Au NPs formed by alternative reduction methods have solely focused on the change in particle size for the initial reaction duration, where at best, the reaction was monitored for a few hours.[28–30]

The phenomenon of an average particle size decrease is uncommon as it opposes reductions in interfacial free energy gained by the particle from increase in size.[31] However, by refluxing polydisperse Au NP solutions in the presence of surface active ligands, Prasad *et al.* observed a similar phenomenon, with an overall reduction in NP size and a conversion to monodispersity.[32,33] This inverse Ostwald ripening process, termed digestive ripening, occurred after just 90 min of reflux.

In this paper we present the extended time evolution of citrate formed Au NPs stored in both light and dark. From monitoring the change in SPR centre, it was found that NP sizes slowly decreased from their Ostwald ripened maxima and levelled out over subsequent days of standing, regardless of being in the light or dark, with a decrease in average size from *ca.* 15 to 12 nm. A time evolution narrowing of the particle size distribution from the tightening of SPR bands as well as dynamic light scattering measurements was seen. Notably we show after removing the free citrate and auric acid from the solution when still purple in colour by centrifugation that the system still undergoes this reduction in nanoparticle size to a red solution. We believe that the interactions between the large Au^0 clusters initially formed in solution can lead to the eventual formation of a smaller monodisperse colloid. This phenomenon of inverse-Ostwald growth can be described as digestive ripening. HRTEM images following the progression of the digestive ripening process not only showed an overall size decrease but also a narrowing of the particle size distribution. A mechanism by which digestive ripening proceeds in citrate formed Au NPs will be proposed.

Results and discussion

Gold colloid solutions were prepared by the addition of sodium citrate solution to heated auric acid solutions. Upon addition of citrate all solutions initially displayed a colour change from colourless to lilac. After allowing them to cool with stirring, a relatively fast colour change to light red was also observed after *ca.* 3 min. Although the oil bath that completely encapsulated the reaction flask was heated homogenously with a temperature controlled resistance wire and the citrate added at a consistent rate, the rate of transition from colourless to lilac to red and the depth of final colour differed slightly for each repeat synthesis, in agreement with the chaotic reaction growth mechanism.[34] Over subsequent days the red solutions deepened in colour regardless of light or dark storage. This was tracked by UV-visible absorption spectra and shown to be due to an increase in intensity of the SPR centre. This could indicate that there is either an incomplete initial reduction of auric acid and a subsequent further reaction with excess citrate occurs, or a greater number of smaller NPs are formed from larger NPs due to the digestive ripening of the colloid. A visual example for both light and dark stored solutions of this colour deepening is shown in Fig. 1 for sample A.

Fig. 1 Chronological images of Sample A, a Au NP solution produced *via* a Turkevich citrate reduction removed from heat whilst still purple in colour, and allowed to age in both light and dark storage conditions. Both solutions equally digestively ripened to a deeper red and more monodisperse colloidal solution over a period of days at the same rate.

Time-evolution studies

In the first week, a systematic shift of the SPR centre to lower wavelengths was observed for solutions A–D (light or dark), demonstrating an average size decrease and digestive ripening of NPs in solution. SPR peak maxima increased in absorbance intensity, corresponding to the deeper colour seen by eye (Fig. 1). An eventual narrowing of the SPR peaks was also observed, demonstrating a tightening of the size distribution of NPs in solution. All these phenomena are clearly seen in Fig. 2 from stacked UV-visible absorption spectra for sample A.

Integrating the SPR peaks over the 460–720 nm range quantified the initial increase and levelling of the depth in colour for all solutions. A plot of the SPR peak integrals as well as the SPR centres for both light and dark stored solutions over a 17 day analysis period for sample A is shown in Fig. 3.

The SPR centre decreases systematically from 526–540 nm and subsequently levels out at 522–523 nm for samples A–D, regardless of light or dark storage, clearly demonstrating the mechanism for this digestive ripening is not a light activated or dependent process. Although on Day 1, there were deviations in the position of the SPR centres, after an extended time

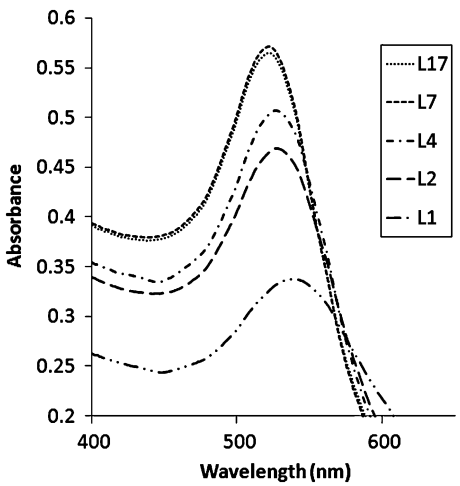

Fig. 2 Stacked UV-visible absorption spectra recorded over the range 400 - 700 nm for selected days over the analysis period of sample A, a Au NP solution produced *via* a Turkevich citrate reduction removed from heat whilst still purple in colour. The systematic decrease in SPR centre to shorter wavelength is observed, indicative of an average NP size decrease in solution and a digestive ripening effect. L1 - L17 represent a light stored solution from days 1 to 17.

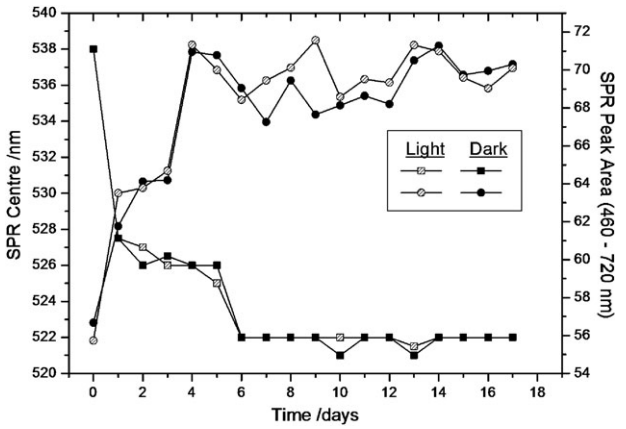

Fig. 3 A daily plot of SPR centre and SPR peak integral (over the range 460 - 720 nm) over the total analysis period for both light and dark stored solutions of sample A, a Au NP solution produced *via* a Turkevich citrate reduction removed from heat whilst still purple in colour.[21] No precipitation nor turbulence was observed in the solution.

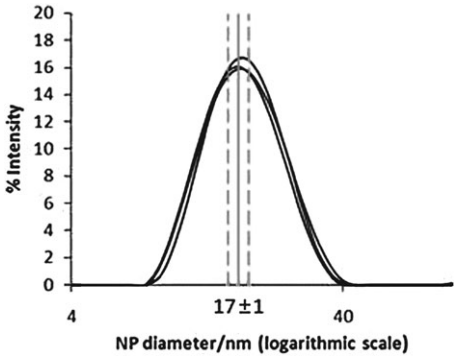

Fig. 4 Photon Correlation Spectroscopy (PCS) measurements of all three runs on light stored sample D, a Au NP solution produced *via* a Turkevich citrate reduction removed from heat whilst still purple in colour; where the mean NP diameter was calculated from the average of the peak maxima and the standard deviation taken as the error.

period of digestive ripening, all SPR bands maxima fall within 1 nm from each other. Although best efforts were made to conduct the synthesis in the most reproducible way, these initial differences in SPR position were always seen. Nonetheless, subsequent ripening causes an eventual movement of all SPR bands to virtual equivalence in monodispersity (SPR broadness) and size (SPR centre). Additionally, the SPR peak areas increase from around 55–57 (arbitrary units) and level out at around 69–70 (arbitrary units), once again for both light and dark stored samples (Table 1). After a further one month storage of both light and dark samples, partial precipitation of colloidal gold occurred in some samples; however, SPR centres only deviated by ±1 nm (if at all) with peak areas ranging from 66 to 72 (arbitrary units), consistent with what was previously seen.

The hydrodynamic diameters of all four light stored Au NP solutions A–D were calculated *via* photon correlation spectroscopy (PCS) measurements on a Zetasizer 3000, conducted in plastic cuvettes at 25 °C. The experiment was carried out three times and the values reported in Table 1 are averages of the central position of the peak maxima (Fig. 4). Insufficient correlation in Zetasizer measurements for samples analyzed on Day 1 inhibited NP diameters to be calculated by PCS. This was attributed to the wide size distributions seen from their SPR width. The PCS measurements indicate the hydrodynamic diameters of the nanoparticles. These were approximately double that indicated by HRTEM measurements.

High resolution transmission electron microscopy (HRTEM) was carried out on light stored sample A at Days 1, 4, 7 and 12 (Fig. 5) using a Joel 4000EX HREM instrument, prepared by evaporating solution droplets on lacey carbon coated copper discs. Au NP diameters were calculated from the resulting images, whereby an average particle size and associated error were extracted (Table 1). Au NPs of significantly different average size and distribution were observed for sample A at Day 1 (Fig. 5(a)) and Day 12 (Fig. 5(d)). An ~20% decrease in NP diameter over the ripening period from an average of 15 ± 6 nm to 12 ± 2 nm confirmed the digestive ripening seen from UV-visible absorbance SPR shifts, with the average and table of probable indifference shown in Fig. 6. The Welch's *t*-test demonstrated the high probability in time evolution averages being significantly different from each other (Fig. 6). A decrease in the NP size distribution, indicated by a sizeable reduction in the standard deviation of sizes, demonstrated a time evolution towards monodispersity and correlated with the narrowing of the SPR band seen spectroscopically (Fig. 2).

In order to assess whether the inverse-Ostwald nanoparticle growth was dependent upon the presence of excess un-reacted citrate, sample E was separated in two equal volumes and vigorously centrifuged to force the Au NPs to the bottom of a clear solution. The excess citrate dispersed in aqueous solution above the resting gold was replaced with distilled water in one of the samples. The process of centrifugation was repeated a further two times to make sample E^-. After re-dispersion of the NPs by rapid vortex, causing the solution to become purple once more, the time evolution of both samples E and E^-

Table 1 Table of information collected from UV-visible absorption spectroscopy, calculated particle diameters from the equation formulated by Haiss *et al.*, photon correlation spectroscopy (PSC) and high resolution transmission electron microscopy (HRTEM) for light stored samples A–D, Au NP solutions produced *via* a Turkevich citrate reduction removed from heat whilst still purple in colour

	SPR centre/nm		SPR area (Abs)/nm		Calculated diameter/nm		PCS/nm	TEM/nm			
Sample	Day 1	Day 21	Day 1	Day 21	Day 1	Day 21	Day 21	Day 1	Day 4	Day 7	Day 12
A	538	522	56	69	64	6	19 ± 3	15.2 ± 6.3	14.3 ± 4.9	12.3 ± 1.7	12.4 ± 1.9
B	535	522	25	65	57	10	23 ± 2	—	—	—	—
C	526	522	70	69	35	9	20 ± 2	—	—	—	—
D	540	523	64	69	67	10	17 ± 1	—	—	—	—

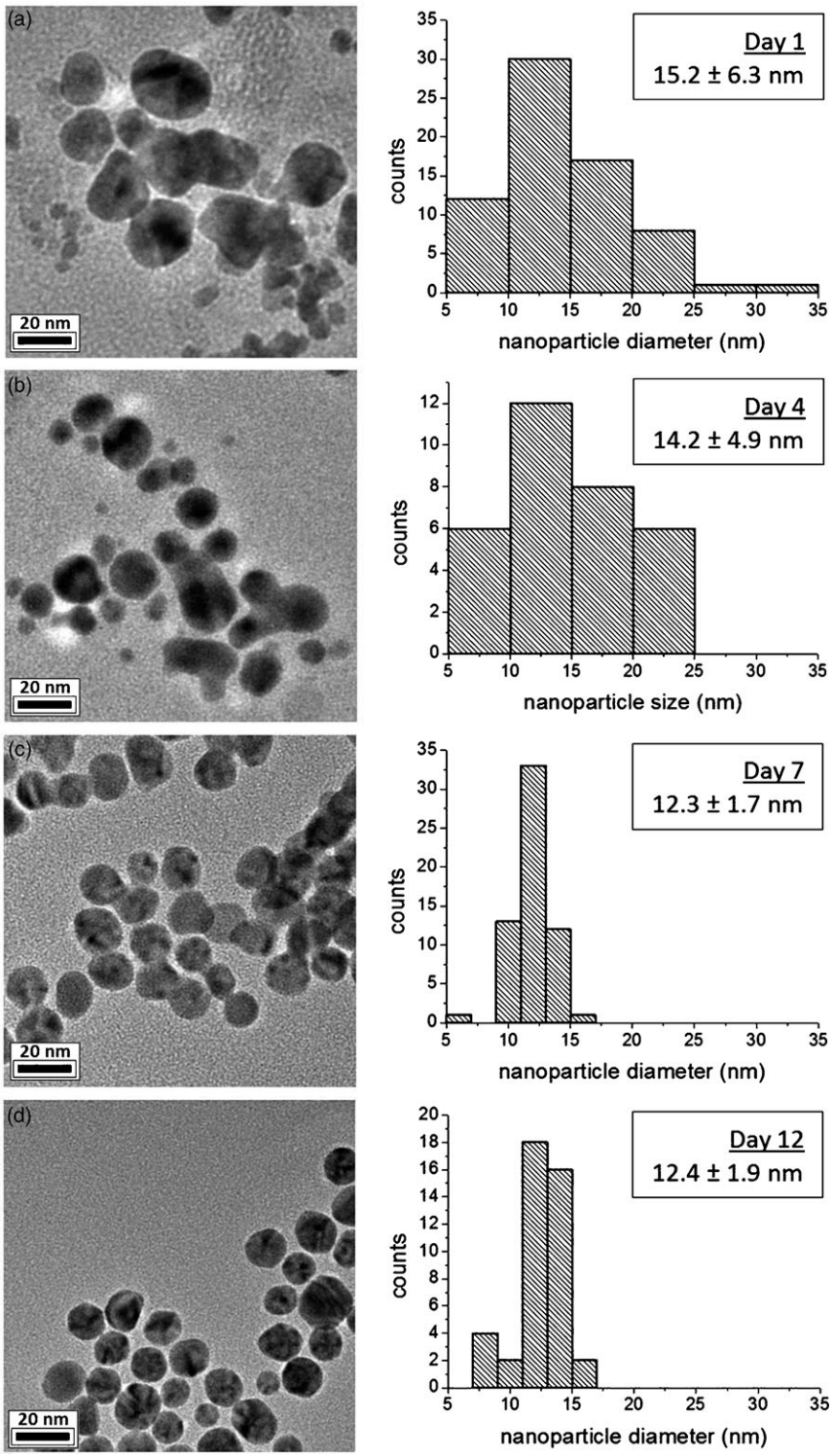

Fig. 5 HRTEM images of light stored Sample A, a Au NP solution produced *via* a Turkevich citrate reduction removed from heat whilst still purple in colour, at (a) Day 1 and (b) Day 4 (c) Day 7 and (d) Day 12 with a histogram plot of the size information directly shown.

was monitored by UV-visible spectroscopy; the changes in SPR centres are shown in Fig. 7. A systematic shift and levelling in the SPR centre to lower wavelengths was indicative of an equivalent digestive ripening process occurring in both samples E and E^{-}, analogous to non-centrifuged samples A–D. HRTEM images of sample E^{-} at Day 1 and 12 are shown in Fig. 8. A similar pattern of size decrease and distribution narrowing to sample A is observed, with the average size decreasing from 14–11 nm. This demonstrated the independence of digestive ripening to the presence of excess citrate and un-reacted auric acid and indicated that the inverse-Ostwald growth was likely due to no further

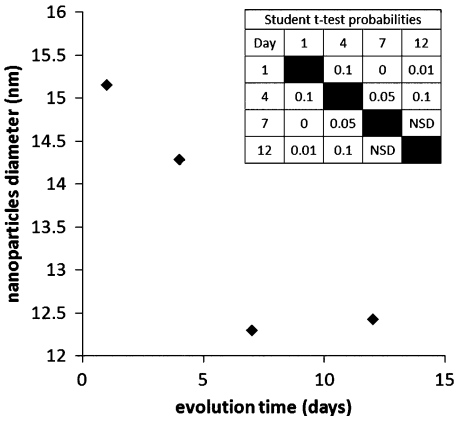

Fig. 6 A graph of average nanoparticle sizes of Sample A with a table of probability of significant difference between ripening periods calculated using a Welch's t-test; a Au NP solution produced *via* a Turkevich citrate reduction removed from heat whilst still purple in colour, taken from HRTEM images of solution droplets when allowed to ripen over a 12 day period. NSD denotes no significant difference between the sample averages.

capping reaction and merely to interactions between the larger Au^0 clusters initially formed in solution.

Although the Au NP diameters, derived *via* the Haiss formulation[24] from SPR centres, were approximately double what was seen in TEM images pre-ripening (Day 1), the difference between prediction and observation post-ripening was minimal (Table 1). This would indicate that the nanoparticles initially formed in solution tended to agglomerate, as indicated in HRTEM images (Fig. 5(a)). Even though NP diameters calculated from UV-visible absorption data post-ripening were of the same order to what was seen from HRTEM images, they tended to underpredict the size. In addition, when predicting larger Au NP diameters, the equation seemingly

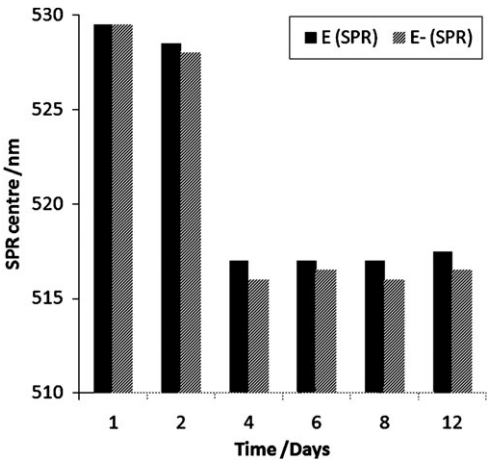

Fig. 7 A plot of SPR peak centre (nm) and for Sample E and the tri-centrifuged and purified Sample E^-, a pair of Au NP solutions produced *via* a Turkevich citrate reduction removed from heat when purple in colour. The systematic shifting of SPR centre to lower wavelengths in both samples was indicative of a digestive ripening phenomenon and not an extended citrate reaction or reagent-product charge in-balance, given the excess citrate and auric acid removal from Sample E^-.

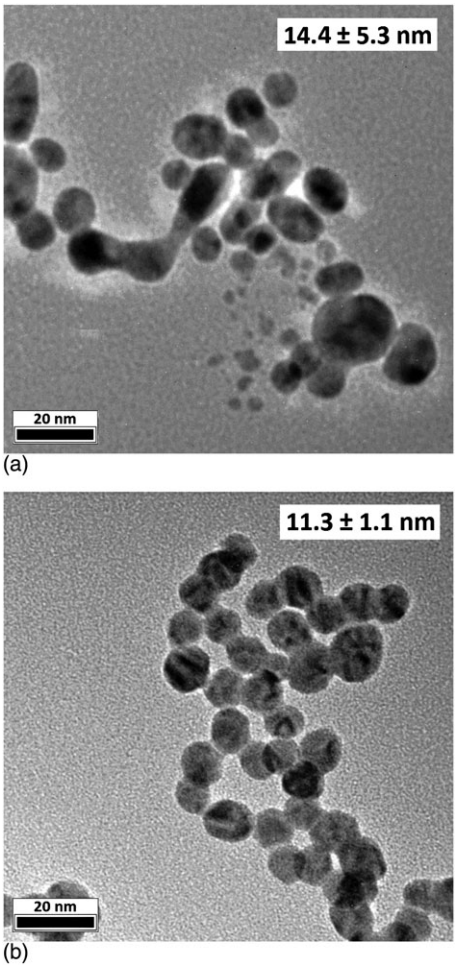

Fig. 8 HRTEM images of Sample E^-; a Au NP solution produced *via* a Turkevich citrate reduction, removed from heat whilst still purple in colour and then tri-centrifuged and purified to remove any excess un-reacted reagents at (a) Day 1 and (b) Day 12.

breaks down altogether and can only be treated as a guide. While post-ripened Au NP diameters predictions were in line with what was seen in TEM images, they were significantly different from those determined *via* PCS, which seemingly over-represents Au NP size given that a hydrodynamic size is measured.[35]

It was evident that initial SPR centres position and areas attained from UV-visible spectroscopy did not directly correlate and furthermore demonstrated that the degree of initial Au NP formation, which differed quite substantially between samples, had no effect on the final NP size achieved after allowing particles to sufficiently digestively ripen. However if the solutions are allowed to sufficiently age effectively, near monodisperse nanoparticles are obtained. Notably this synthesis did not give rise to rod-shape nanoparticles. After allowances for aging most of the particles were near spherical in shape although the occasional triangular facet was noted.

Collective assessment of UV-visible, PCS and HRTEM data clearly shows that a gradual NP size decrease to an optimum as well as an increase in the monodispersity of sizes occurred for all five samples A–E. The rarity of this phenomenon is unsurprising given the process avoids the reduction of

interfacial free energy gained from particle aggregation; however by considering the electrostatic interactions between particles computational models have accounted for this behaviour for systems under reflux.[31] Some groups have exploited this process in creating monodisperse Au NP solutions by refluxing polydisperse colloids with a series of alkylthiols invoking digestive ripening. Given the popularity of the simple Turkevich method used in this study for Au NP formation it is surprising that the ramifications of this inverse Ostwald growth have gone unnoticed. However, the rate of heating, cooling and citrate addition used in our procedures could favour digestive ripening.

Experimental

Synthesis

All glassware was washed with aqua regia (3HCl : 1HNO_3) and rinsed with copious amounts of deionised water. Stock solutions labelled A and B were made up; solution A consisting of $HAuCl_4 \cdot 3H_2O$ (170 mg) dissolved in 100 cm^3 deionised water (5 mM) and solution B consisting of $Na_3C_6H_5O_7 \cdot 2H_2O$ (250 mg) dissolved in 50 cm^3 deionised water (20 mM). A 1 cm^3 aliquot of solution A was dissolved in 18 cm^3 of deionised water and uniformly heated in an oil bath with constant stirring. When the solution began to boil, 1 cm^3 of solution B was allowed to fall drop wise through a frit over a period of 6 min. After a characteristic colour change to lilac was observed the solution was removed from the oil bath and allowed to cool to room temperature whilst being stirred. Solutions were not refluxed as this encouraged rapid digestive ripening of the colloid, pushing the reaction and evolution to completion before a thorough analysis of the phenomenon could be studied.

Five repeat Au NP solutions, labelled sample A–E, were synthesized in this manner.

Analysis

Solutions A–D were divided into two portions: one was stored in the light and the other in the dark. Changes in SPR and colour were monitored daily by UV-visible spectroscopy using a PerkinElmer Lambda 25 UV/VIS spectrometer and digital images taken using a Kodak C813 digital camera, respectively, for three weeks. Subsequently particle diameters of all four solutions stored in the light were calculated *via* photon correlation spectroscopy (PCS) on a Zetasizer 3000 (Malvern, UK). Particle diameters of light stored solution A were also directly measured on Days 1, 4, 7 and 12 to progressively monitor the digestive ripening process using a Joel 4000EX HREM high resolution transition electron microscope (HRTEM), prepared by evaporating solution droplets on lacey carbon coated copper discs. Solution E, pre-ripening (Day 1), was also divided into two 9 cm^3 portions and both centrifuged on a Beckman Coulter Avanti Centrifuge J-26 XP at 20 000 rpm ($\sim$48 000 $\times$ g) causing the NPs to rest at the bottom of the solution. Most of the excess un-reacted citrate was removed from one solution and replaced with distilled water (7 cm^3). This process was repeated a further two times. Both solutions were vortexed in order to re-disperse the NPs at rest, once more forming homogenous pink coloured solutions, and their subsequent evolution monitored by UV-visible spectroscopy.

Conclusion

A simple Turkevich method was used to produce four Au NP solutions, stored either in the light or dark. Daily monitoring of the solutions with UV-visible absorption spectroscopy identified a gradual time evolutionary shift in the SPR centre of solutions to lower wavelengths, indicating a decrease in particle size. An eventual stabilization of SPR centres at approximately 522 nm for all samples, both light and dark, demonstrated the independence of lighting conditions upon the optimisation mechanism of this inverse Ostwald growth. A size decrease from roughly 15 nm at synthesis to around 11–12 nm at stabilization was confirmed by HRTEM imaging. The decrease in size was observed for both solutions with excess un-reacted auric acid and citrate present and purified solutions (citrate and auric acid completely removed), indicating that solely interactions between larger Au^0 clusters that initially form in solution cause the progressive shrinking reaction over several days, deemed digestive ripening. An overall increase in the monodispersity of sizes after the ripening period was not only indicated by a tightening of the SPR bands but also clearly observed in HRTEM images and size analysis. We believe this to be the first time digestive ripening has been observed for Turkevich prepared Au NPs. This study has shown that Au NPs of increasingly consistent size can be obtained *via* the Turkevich method by simply harvesting for a pre-determined time period.

Acknowledgements

IPP wishes to thank the RS/Wolfson Trust for a merit award, and Josie Goodhall and Jawaad Darr for help with the Zetasizer measurements. The EPSRC is thanked for funding the access to the TEM instruments in Oxford Materials under the Materials Equipment Access scheme, grant reference: EP/F01919X/1.

References

1 G. Walters and I. P. Parkin, *J. Mater. Chem.*, 2009, **19**, 574.
2 M. C. Ferrara, L. Mirenghi, A. Mevoli and L. Tapfer, *Nanotechnology*, 2008, **19**, 365706.
3 L. Armelao, D. Barreca, G. Bottaro, A. Gasparotto, C. Maccato, C. Maragno, E. Tondello, U. L. Stangar, M. Bergant and D. Mahne, *Nanotechnology*, 2007, **18**, 375709.
4 A. Ito, H. Masumoto and T. Goto, *Mater. Trans., JIM*, 2003, **44**, 1599.
5 R. G. Palgrave and I. P. Parkin, *Chem. Mater.*, 2007, **19**, 4639; A. Mills, S. K. Lee, A. Lepre, I. P. Parkin and S. A. O'Neill, *Photochem. Photobiol. Sci.*, 2002, **1**, 865; W. B. Cross, I. P. Parkin, S. A. O'Neill, P. A. Williams, M. F. Mahon and K. C. Molloy, *Chem. Mater.*, 2003, **15**, 2786; S. A. O'Neill, I. P. Parkin, R. J. H. Clark, A. Mills and N. Elliot, *J. Mater. Chem.*, 2003, **13**, 56; W. B. Cross and I. P. Parkin, *Chem. Commun.*, 2003, 1696; I. P. Parkin and R. G. Palgrave, *J. Mater. Chem.*, 2004, **14**, 2864.
6 R. G. Palgrave and I. P. Parkin, *J. Am. Chem. Soc.*, 2006, **128**, 1587.
7 R. Binions, C. Piccirillo, R. G. Palgrave and I. P. Parkin, *Chem. Vap. Deposition*, 2008, **14**, 33.

8 S. Nath, C. Kaittanis, A. Tinkham and J. M. Perez, *Anal. Chem.*, 2008, **80**, 1033.
9 J. Gil-Tomas, S. Tubby, I. P. Parkin, N. Narband, L. Dekker, S. P. Nair, M. Wilson and C. Street, *J. Mater. Chem.*, 2007, **17**, 3739.
10 S. Perni, C. Piccirillo, J. Pratten, P. Prokopovich, W. Chrzanowski, I. P. Parkin and M. Wilson, *Biomaterials*, 2009, **30**, 89.
11 C. Yu, H. Nakshatri and J. Irudayaraj, *Nano. Lett.*, 2007, **7**, 2300.
12 M. Li, Y. Lin, C. Wu and H. Liu, *Nucleic Acids Res.*, 2005, **33**, 184.
13 X. Qian and S. M. Nie, *Chem. Soc. Rev.*, 2008, **37**, 912.
14 K. Lee and M. A. El-Sayed, *J. Phys. Chem. B*, 2006, **110**, 19220.
15 J. E. Park, M. Atobe and T. Fuchigami, *Ultrason. Sonochem.*, 2006, **13**, 237.
16 M. A. Ortega, L. Rodriguez, J. Castillo, V. Piscitelli, A. Fernandez and L. Echevarria, *J. Opt. A: Pure Appl. Opt.*, 2008, **10**, 104024.
17 D. Werner, S. Hashimoto, T. Tomita, S. Matsuo and Y. Makita, *J. Phys. Chem. C*, 2008, **112**, 16801.
18 N. Basu, R. Bhattacharya and P. Mukherjee, *Biomed. Mater.*, 2008, **3**, 034105.
19 R. G. Palgrave and I. P. Parkin, *Gold Bull.*, 2008, **41**, 66.
20 M. Brust, M. Walker, D. Bethell, D. J. Schiffrin and R. Whyman, *J. Chem. Soc., Chem. Commun.*, 1994, **7**, 801.
21 J. Turkevich, P. C. Stevenson and J. Hillier, *Discuss. Faraday Soc.*, 1951, **11**, 55.
22 G. Schneider and G. Decher, *Langmuir*, 2008, **24**, 1778.
23 C. L. Nehl and J. H. Hafner, *J. Mater. Chem.*, 2008, **18**, 2415.
24 W. Haiss, N. Thanh, J. Aveyard and D. Fernig, *Anal. Chem.*, 2007, **79**, 4215.
25 X. Liu, M. Atwater, J. Wang and Q. Huo, *Colloid Surf., B*, 2007, **58**, 3.
26 J. Kimling, M. Maier, B. Okenve, V. Kotaidis, H. Ballot and A. Plech, *J. Phys. Chem. B*, 2006, **110**, 15700.
27 R. A. Oriani, *Acta Metall.*, 1964, **12**, 1399; B. Rodriguez-Gonzalez, P. Mulvaney and L. M. Liz-Marzan, *Z. Phys. Chem. (Munich)*, 2007, **221**, 415; M. K. Chow and C. F. Zukoski, *J. Colloid Interface Sci.*, 1994, **165**, 97.
28 W. Hao, W. Yang, W. Huang, G. Zhang and Q. Wu, *Mater. Lett.*, 2008, **62**, 3106.
29 H. K. M. Tanaka, M. McIntire and R. Castillo-Garza, *Microporous Mesoporous Mater.*, 2005, **85**, 374.
30 R. Salvati, A. Longo, G. Carotenuto, S. De Nicola, G. P. Pepe, L. Nicolais and A. Barone, *Appl. Surf. Sci.*, 2005, **248**, 28.
31 D. Lee, S. Park, J. K. Lee and N. Hwang, *Acta Mater.*, 2007, **55**, 5281; S. I. Stoeva, A. B. Smetana, C. M. Sorensen and K. J. Klabunde, *J. Colloid Interface Sci.*, 2007, **309**, 94.
32 B. L. V. Prasad, S. I. Stoeva, C. M. Sorensen and K. J. Klabunde, *Chem. Mater.*, 2003, **15**, 935.
33 B. L. V. Prasad, S. I. Stoeva, C. M. Sorensen and K. J. Klabunde, *Langmuir*, 2002, **18**, 7515.
34 S. Kumar, K. S. Gandhi and R. Kumar, *Ind. Eng. Chem. Res.*, 2007, **46**, 3128.
35 D. Jankovic, T. Maksin, D. Djokic, S. Milonjic, N. Nikolic, M. Mirkovic and S. Vranjes-Djuric, *J. Microsc.*, 2008, **232**, 601.